Magnetic and electronic properties of strontium hexaferrite $SrFe_{12}O_{19}$ from first-principles calculations

2003 J. Phys.: Condens. Matter 15 6229

(http://iopscience.iop.org/0953-8984/15/36/311)

INSTITUTE OF PHYSICS PUBLISHING JOURNAL OF PHYSICS: CONDENSED MATTER

J. Phys.: Condens. Matter **15** (2003) 6229–6237 PII: S0953-8984(03)63135-8

Magnetic and electronic properties of strontium hexaferrite $SrFe_{12}O_{19}$ from first-principles calculations

C M Fang[1], F Kools[1], R Metselaar[1], G de With[1] and R A de Groot[2]

[1] Laboratory of Solid State and Materials Chemistry, Eindhoven University of Technology, Post Box 513, 5600 MB Eindhoven, The Netherlands
[2] Electronic Structure of Materials, Research Institute for Materials, Toernooiveld 1, 6525 ED Nijmegen, The Netherlands

Received 8 May 2003, in final form 16 July 2003
Published 29 August 2003
Online at stacks.iop.org/JPhysCM/15/6229

Abstract

The magnetic and electronic structure of strontium hexaferrite $SrFe_{12}O_{19}$ has been investigated using density functional theory within the local spin density approximation. The calculations show that in this ferrite all the Fe^{3+} ions are fully spin polarized with $S = 5/2$. The electronic structure of this ferrite is strongly influenced by the exchange interactions between the iron ions. The most stable form of the ferrite is a ferrimagnet with the Fe^{3+} ions at the 4f sites having their spin polarization anti-parallel to the rest of the Fe^{3+} ions, in agreement with Gorter's prediction. The ferrite $SrFe_{12}O_{19}$ is calculated to be a semiconductor with both the top of the valence band and the bottom of the conduction band being dominated by Fe 3d states. A strong anisotropy was found for the conductive charge carriers. The calculated results are in good agreement with the available experimental data.

1. Introduction

Strontium hexaferrite $SrFe_{12}O_{19}$ has been a subject of continuous interest and intensive study for several decades due to the fact that this compound has been the work horse of the permanent magnet market since shortly after its discovery in the 1950s [1, 2]. $SrFe_{12}O_{19}$ has also been investigated as a medium for magnetic recording and magneto-optical recording and for long (millimetre)-wave devices. From the crystal chemistry point of view this ferrite has an interesting and complex magnetoplumbite-type structure [3], in which the iron ions are coordinated tetrahedrally (FeO_4), trigonal bipyramidally (FeO_5) and octahedrally (FeO_6) by oxygen ions. The super-exchange interactions of the Fe ions in this complex structure are an interesting subject [4].

0953-8984/03/366229+09$30.00

Studies on hexaferrite $SrFe_{12}O_{19}$ deal mainly with the preparation, characterization and measurements of physical properties. Recently attention has been paid to the physical properties of $SrFe_{12}O_{19}$ with pair doping, such as a La–Co pair to replace a Sr–Fe pair [5, 6]. Magnetic measurements showed that the hexaferrite $SrFe_{12}O_{19}$ is a ferrimagnetic compound with $S = 5/2$ for every Fe ion. Several models for the magnetic ordering of these Fe^{3+} ions in the ferrites have been proposed [7]. In the 1950s Gorter predicted that the iron ions at the trigonal bipyramidal (2b) and octahedral (2a, 12k) sites have their spin orientation anti-parallel to that of the iron ions at the 4f sites [8–10]. $SrFe_{12}O_{19}$ also shows a strong anisotropy in electric conductivity as well as magnetic orientation [11, 12]. In spite of the importance of the hexaferrite, there are almost no theoretical publications about the electronic structure and magnetic properties. Using *ab initio* linear muffin-tin orbital calculations in the tight binding approximation (LMTO-TB) and semi-empirical extended Hückel theory (EHT), Zainullina *et al* [13] recently studied the electronic structure, chemical bonding and ion conductivity of lead hexaferrite $PbFe_{12}O_{19}$, although the magnetic structure was not investigated. In the present paper results of first-principles calculations for the electronic structure and magnetic ordering of the strontium hexaferrite $SrFe_{12}O_{19}$ are reported using the localized spherical wave (LSW) method employing density functional theory (DFT) within the spin-polarized local density approximation (SP-LDA). The information obtained here is not only useful for obtaining a good understanding for strontium hexaferrite $SrFe_{12}O_{19}$, but also for the related hexaferrites $MFe_{12}O_{19}$ (M = Ba and Pb), as well as for improvements in the physical properties of these compounds [6, 14].

2. Crystal structure of the hexaferrite $SrFe_{12}O_{19}$

The hexaferrite $SrFe_{12}O_{19}$ was first prepared by Adelsköld in 1938 [3]. He also determined the crystal structure of this compound to be iso-structural with magnetoplumbite. Later structural refinements for strontium hexaferrite $SrFe_{12}O_{19}$ have confirmed his determination [9, 15, 16]. Hexaferrite $SrFe_{12}O_{19}$ is hexagonal with space group $P6_3/mmc$. The lattice parameters measured by Kimura *et al* [16] are $a = 0.588\,36$ nm and $c = 2.303\,76$ nm at room temperature. There are two formula units in a unit cell. As shown in figure 1, the oxygen atoms are close packed with the Sr and Fe ions in the interstitial sites. There are ten layers of oxygen atoms along the c axis. The structure is built up from smaller units: a cubic block S, having the spinel-type structure, and a hexagonal block R, containing the Sr ions. The iron atoms are positioned at five crystallographically different sites, as shown in table 1. The coordination of the Fe ions in the hexaferrite is complicated and unique (table 2). The Fe atoms at 2a are octahedrally coordinated with equal Fe–O distances, while the octahedrally coordinated Fe ions at 4f2 and 12k have different Fe–O interatomic distances, from about 0.185 to 0.237 nm. The Fe atoms at 4f1 are tetrahedrally coordinated by oxygen, while the Fe at 2b sites are coordinated by five oxygen ions. There are also short Fe–Fe distances in the structure. The Fe atoms at 4f2 sites have Fe–Fe distances as short as about 0.27 nm. The Fe ions at 12k sites form a network with every Fe connected to four other Fe ions in the same layer with Fe–Fe distances of about 0.29–0.30 nm [16].

Some insight into the bonding of Fe in $SrFe_{12}O_{19}$ can be obtained using the concept of bond valence [17]. The bond valence V_i is calculated from the relation: $V_i = \exp[(d_o - d_i)/b]$, where d_i is the distance between the atoms of bond i and $b = 0.37$ is a universal constant. The d_o is 0.1759 nm for Fe–O [18]. The total bond valence or oxidation state V of an atom is calculated by summing over all neighbouring atoms $V = \sum V_i$. The calculated bond valences are given in table 2. The Fe ions at the 4f1 and 2b sites have bond valences (about 2.8), somewhat smaller than that of the other iron ions (about 3.0–3.1).

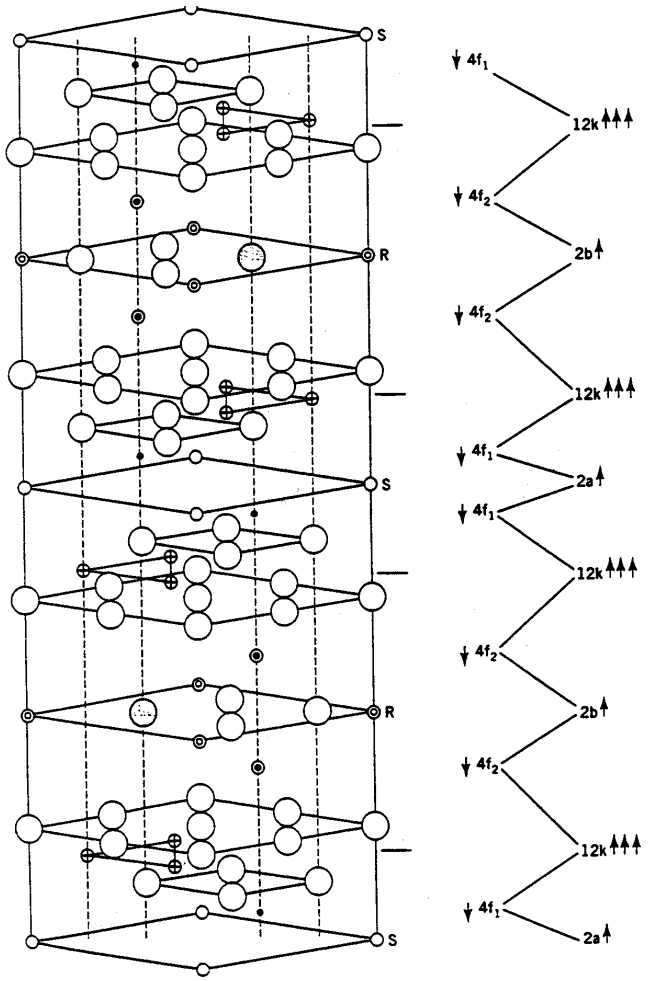

Figure 1. The schematic structure (left) of the hexaferrite $SrFe_{12}O_{19}$ with Gorter's magnetic ordering (right). The large open circles are oxygen ions, the large broken circles are Sr ions; small circles with a cross inside represent Fe ions at 12k, small circles containing a filled circle inside represent Fe ions at 4f2, small unfilled circles represent Fe ions at 4f1, filled small circles represent Fe ions at 2a and small circles with a unfilled circle inside represent Fe ions at 2b. The magnetic structure suggested by Gorter is shown on the right, where the arrows represent the direction of spin polarization.

3. Details of calculations

First-principles band structure calculations were performed for the hexaferrite $SrFe_{12}O_{19}$ with the LSW method [19] using a scalar-relativistic Hamiltonian. We used spin-polarized local-density exchange–correlation potentials (SP-LDA) [20] inside space-filling, and therefore overlapping, spheres around the atomic constituents. The self-consistent calculations were carried out including all core electrons. We performed iterations with 191 $\boldsymbol{k}$ points distributed uniformly in an irreducible part of the Brillouin zone (BZ), corresponding to a volume of the BZ per $\boldsymbol{k}$ point of less than 1×10^{-6} Å^{-3}. Self-consistency was assumed when the changes in the local partial charges in each atomic sphere decreased to the order of 1×10^{-5}.

Table 1. Coordinates of atoms and some calculated results for strontium hexaferrite $SrFe_{12}O_{19}$ of Gorter's form. Space group $P63/mmc$, $a = 0.588\,36$ nm and $c = 2.303\,76$ nm [16].

Atom	Wyckoff site	Symmetry	Coordinates of atoms	RWS (nm)	Charge (electrons)	Magnetic moment (μ_B)
Sr	2d	$\bar{6}m2$	1/3, 2/3, 0.75	0.19	+0.44	0.00
Fe(1)	2a	$\bar{3}m$	0, 0, 0	0.09	+2.65	4.11
Fe(2)	2b	$\bar{6}m$	0, 0, 1/4	0.09	+2.83	3.95
Fe(3)	4f1	$3m$	1/3, 2/3, 0.027 18	0.09	+3.09	−3.88
Fe(4)	4f2	$3m$	1/3, 2/3, 0.190 91	0.09	+2.86	−3.79
Fe(5)	12k	m	0.168 86, 0.337 72, 0.890 83	0.09	+2.78	4.06
O(1)	4e	$3m$	0, 0, 0.1514	0.14	−1.84	0.39
O(2)	4f	$3m$	0, 0, 0.9446	0.14	−1.48	0.09
O(3)	6h	mm	0.1819, 0.3639, 1/4	0.14	−1.50	0.07
O(4)	12k	m	0.1564, 0.3127, 0.052 52	0.14	−1.75	0.13
O(5)	12k	m	0.5039, 0.0078, 0.150 92	0.14	−1.862	0.23
V(1)[a]	6g	$2/m$	1/2, 0, 0	0.11	−0.60	−0.07
V(2)[a]	4f	$3m$	1/3, 2/3, 0.0993	0.11	−0.54	−0.08
V(3)[a]	4f	$3m$	1/3, 2/3, 0.6294	0.06	−0.15	0.00
Total					0.0	40

[a] V denotes an empty site.

Table 2. The important interatomic distances and chemical bonding of Fe ions in strontium hexaferrite $SrFe_{12}O_{19}$ [16].

Bond	Distances (nm)	Total valence bond
Fe(1)–O(4)	0.2001 (6×)	3.12
Fe(2)–O(1)	0.2272 (2×)	2.82
Fe(2)–O(3)	0.1854 (3×)	
Fe(3)–O(2)	0.1901 (1×)	2.75
Fe(3)–O(4)	0.1896 (3×)	
Fe(4)–O(3)	0.2058 (3×)	3.07
Fe(4)–O(5)	0.1963 (3×)	
Fe(5)–O(1)	0.1977 (1×)	3.02
Fe(5)–O(2)	0.2085 (1×)	
Fe(5)–O(4)	0.2112 (2×)	
Fe(5)–O(5)	0.1923 (2×)	

In the construction of the LSW basis [19, 21, 22], the spherical waves were augmented by solutions of the scalar-relativistic radial equations indicated by the atomic symbols 5s, 5p for Sr; 3d, 4s, 4p for Fe, and 2s and 2p for O. The internal l summation used to augment a Hankel function at surrounding atoms was extended to $l = 2$, resulting in the use of 3d/4d orbitals for O/Sr, and to $l = 3$, resulting in the use of 4f orbitals for Fe. The Wigner–Seitz radius employed in the calculations is about 0.14 nm for O, 0.09 nm for Fe and 0.19 nm for Sr. These radii of the spheres are close to the ionic radii [23]. Because the crystal of this hexaferrite is not very densely packed, it is necessary to include empty spheres (V) in the calculations. The functions 1s and 2p, and 3d as an extension, were used for the empty spheres.

4. Magnetic ordering of $SrFe_{12}O_{19}$

For the magnetic ordering of ferrites, there are several possibilities [7]. Gorter [1, 8] predicted that the hexaferrites $SrFe_{12}O_{19}$, as well as $BaFe_{12}O_{19}$ and $PbFe_{12}O_{19}$, are ferrimagnetic

Table 3. Energies, magnetic moments and electrical behaviour for different spin configurations as calculated using the LSW method. Energies are given with respect to the ferromagnetic ordering.

Spin direction of Fe ions in $SrFe_{12}O_{19}$					Energy diff.	Moments	
2a	2b	4f1	4f2	12k	(eV/unitcell)	(μ_B/unitcell)	Status
+	+	+	+	+	0.000	117.33	Metallic
−	+	+	+	+	−1.44	97.18	Metallic
+	−	+	+	+	−1.89	98.89	Metallic
+	+	−	+	+	−3.80	78.14	Metallic
+	+	+	−	+	−4.89	80	Semiconducting
+	+	+	+	−	−6.88	−0.10	Metallic
−	−	+	−	+	−5.51	40	Semiconducting
+	+	−	−	+	−8.66	40	Semiconducting

materials with the magnetic ordering as shown in figure 1. First we calculated the lattice energy of the ferrite $SrFe_{12}O_{19}$ for different magnetic structures. The calculated results, including lattice energy differences to the ferromagnetic ordering, total magnetic moments, conducting behaviour, etc, are listed in table 3.

As shown in table 3, for the types of magnetic order in which only one kind of Fe ions have their spins anti-parallel to the net magnetization, the structure becomes more stable with increasing number of anti-parallel spin Fe sublattices in the system. The structure with octahedral Fe at 4f2 having anti-parallel spins has a lower energy than that with tetrahedral Fe at 4f1 sites. The structure with anti-parallel spins at 12k has a very low energy compared with the ferromagnetic structure.

The calculations also show that structures with anti-parallel spins at 4f2 are calculated to be insulators while other arrangements result in metallic behaviour for the ferrite. Further calculations show that this ferrite is ferrimagnetic with Fe at the 4f1 and 4f2 sites having the magnetic moment anti-parallel to the rest of the Fe atoms. This result is in agreement with the prediction by Gorter in the 1950s [1, 8]. This is also in agreement with the conclusions obtained by Bertaut *et al* [24] using neutron diffraction for the Ba and Sr ferrites. Hereafter we call this stable magnetic ordering Gorter's form.

The calculated results (cohesive energy and magnetic moments, etc) for Gorter's form of $SrFe_{12}O_{19}$ are included in table 3. It is noted that not too much attention should be paid to the absolute numbers, as the charge and magnetic moment on each atom are dependent on the Wigner–Seitz radius of each atom and the existence of empty spheres. However, we can still get useful information. The charge of the Fe ions is close to +3. Local moments for the Fe ions are about 5 μ_B. The total magnetic moment is 40 μ_B/unit cell, indicating $S = 5/2$ (high spin) for every Fe ion. The oxygen ions have a charge close to -2. Therefore, the ionic model for this ferrite is valid to a first approximation. Furthermore, as shown in table 1, the calculations also showed that among the five different Fe^{3+} ions, at an Fe(1) site there is the smallest number of electrons (about 2.65 electrons) while there is the largest number of electrons at the F(3) site (3.09 electrons), which is in agreement with the bond valences in table 2.

5. Electronic structure of $SrFe_{12}O_{19}$

The calculated partial density of states (DOS) of every Fe and the total DOS near the Fermi level (which is set at the top of the valence band) for Gorter's form of $SrFe_{12}O_{19}$ are shown in figure 2. The valence band, which is composed of mainly O 2p and Fe 3d states, has a total

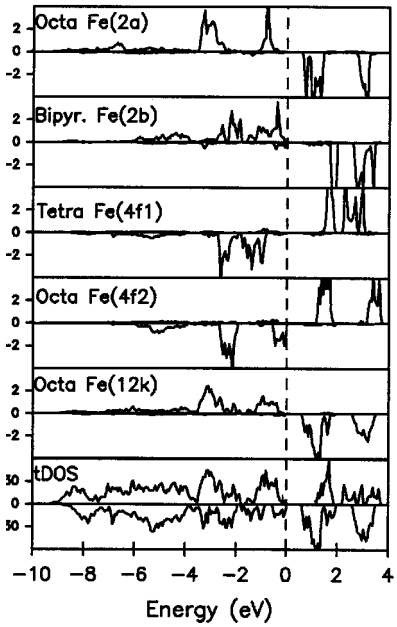

Figure 2. Partial DOS of Fe ions and total DOS of hexaferrite $SrFe_{12}O_{19}$ with Gorter's form. The DOS with positive sign represents the density for spin-up electrons, while the DOS with negative sign represents the density for spin-down electrons.

width of 9.0 eV. The lower part (from about −9.0 to −3.8 eV) is dominated by O 2p character, while the upper part (from about −3.8 eV to the Fermi level) is mainly composed of Fe 3d character hybridized with some O 2p states. As shown in figure 2, the crystal field splittings (triplet t_2g and doublet e_g) for the octahedral Fe at 2a, as well as the Fe at 4f2 and 12k, can be easily distinguished, although the position and splitting width of the three kinds of octahedral Fe ions are different due to different Fe–O bondings. The crystal field splitting (doublet e_g and triplet t_2g) for the tetrahedral Fe at 4f1 is also apparent. The crystal splitting of the Fe ions at 2b sites is very complicated due to the trigonal bipyramidal coordination, as well as the super-exchange interactions between the Fe ion at 2b and those at 12k.

To understand the exchange interactions between Fe ions, we compare the partial DOS of the Fe ions and total DOS for the ferromagnetic $SrFe_{12}O_{19}$ (figure 3) with those of Gorter's form (figure 2). The bands in the ferromagnetic form are broader and more distorted compared with those of Gorter's form. There are some important differences, which need to be discussed in detail. For the Fe ions at the 2a sites, the spin-polarization splittings of these Fe ions are almost the same (figures 2 and 3). The total bandwidth of the e_g–t_2g splitting for the Fe ions at the 2a sites in Gorter's form is about 2.9 eV (figure 2), which becomes in the ferromagnetic form about 3.8 eV. These changes are due to the exchange interactions between the Fe ions at 2a sites and those at 4f1 and 4f2 sites. For the spin-up electrons, the bandwidths (3.8 and 4.3 eV for the octahedral Fe at 4f1 and the octahedral Fe at 4f2, respectively) in the ferromagnetic form are much larger than those (1.6 and 2.6 eV) in Gorter's form. In fact the broadness of the band is the cause of the overlap between the valence band and the conduction band for the ferromagnetic form. This originates from the strong exchange interactions between the Fe ions at 2b and 12k sites and those at the 4f1 and 4f2 sites, due to the rather short Fe–Fe distances in the structure [16]. That is the cause of the instability of the ferromagnetic structure of the hexaferrite $SrFe_{12}O_{19}$.

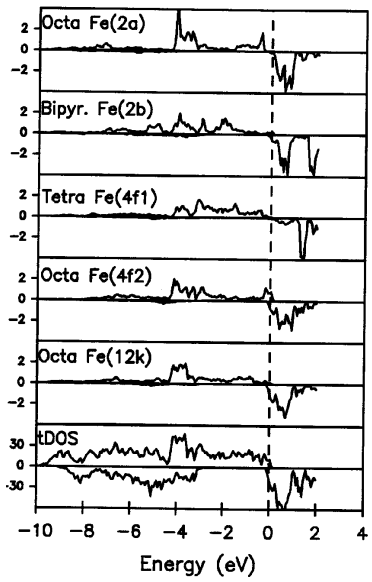

Figure 3. Partial DOS of Fe ions and total DOS of hexaferrite $SrFe_{12}O_{19}$ with ferromagnetic ordering.

The calculations show that both the bottom of the conduction band and the top of the valence band are dominated by Fe 3d states. $SrFe_{12}O_{19}$ is a semiconductor with an energy gap of about 0.6 eV for the spin-down electrons (figure 2).

Figure 4 shows the dispersion curves along the high symmetry lines in the BZ for the spin-up (a) and spin-down (b) electrons of Gorter's form of $SrFe_{12}O_{19}$. The dispersion curves show a strong anisotropy with rather strong dispersion along the directions perpendicular to the c axis (Γ–H, Γ–M, Γ–L and A–L) and very small dispersions along the directions parallel to the c axis (Γ–A, K–H and M–L).

For comparison we calculated the effective band masses for the conductive charge carriers from the dispersion curves of the top of the valence band (holes, h for short) and the bottom of the conduction band (conducting electron, e for short), using the formulae: $1/m^* = (\delta^2\varepsilon/\delta k^2)/\hbar^2$, where ε is the eigenenergy at a k point in the BZ, and $\hbar$ is the Planck quantum constant $h/(2\pi)$. Along the direction perpendicular to the c axis the ferrite has light holes with an effective mass of about 5.4 $m_{e(h)}$ ($m_{e(h)}$ is the mass of a free electron (hole)) and heavy conductive electrons (15.9 m_e), while along the c axis, the ferrite has very heavy holes with effective band mass of about 36.2 $m_{e(h)}$ and relatively light conductive electrons of about 10.2 m_e.

Measurements of the electrical and optical properties of the hexagonal ferrites are scarce. All authors agree that the electrical conductivity in both Ba-, Pb- and Sr-hexaferrite parallel to the c axis is one to two orders lower than perpendicular to this axis [1, 25–27]. According to Baszynski [27] the same holds for the thermoelectric power. It is assumed that electron transport occurs via a hopping mechanism between Fe^{2+} and Fe^{3+} ions. The Fe^{2+} are easily formed due to a small reduction of the ferrite. For instance, in Ba-hexaferrite up to 0.25 wt% Fe^{2+} can be accommodated in the lattice, compensated by oxygen vacancies [28–30]. The anisotropy in the conductivity is attributed to a higher hopping probability in the plane perpendicular to the c axis [27]. In this plane direct electron transfer is possible due to the short Fe–Fe distances and correspondingly large orbital overlap. Parallel to the hexagonal axis electron transfer between Fe^{2+} and Fe^{3+} has to be mediated by O^{2-} ions. Since a detailed analysis of the conductivity and

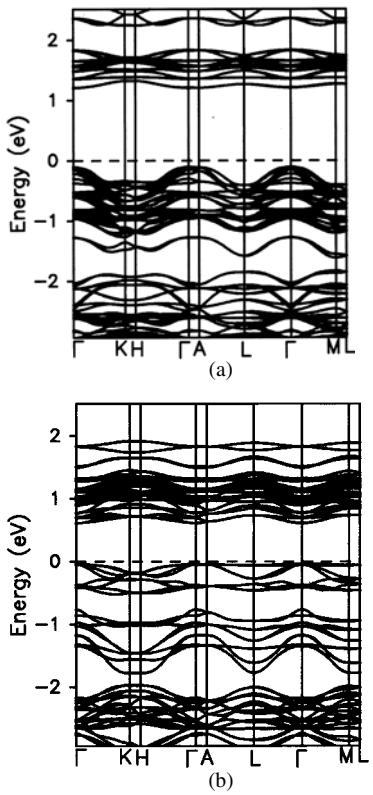

Figure 4. Dispersion curves along the high symmetry lines in the BZ of hexaferrite $SrFe_{12}O_{19}$ for the spin-up (a) and spin-down (b) electrons.

thermopower in terms of extrinsic versus intrinsic behaviour and hopping energy is lacking, a comparison with our band structure calculation is not possible.

The same holds for the optical data. Blazey [1] reported on the reflectivity spectra of $BaFe_{12}O_{19}$ with minima at 2.2, 2.6, 3.9, 4.3 and 4.8 eV. He attributed the first two peaks to internal transitions on tetrahedral iron and the other peaks to charge transfer to octahedral iron. Drews and Jaumann [1] also find a band at about 1.0 eV. No results are available for Sr-hexaferrite. As is known from detailed research of the Kerr effect on spinel type ferrites, the assignment of the large number of bands is very intricate since one has to deal with a mixture of intervalence charge transfer, intersublattice charge transfer and crystal field transitions [29]. We expect that the experimental energy gap of Sr ferrite is larger than the calculated value (0.63 eV) as it is well known that the LDA we employed generally underestimates the energy gap for semiconductors [31]. We expect that our band structure calculations will be useful for a future analysis of the optical spectra of hexagonal ferrites.

6. Conclusions

First-principles band structure calculations with the LSW method have been performed to understand the magnetic and electronic properties of Sr-hexaferrite $SrFe_{12}O_{19}$. The calculations show that the Fe ions are almost fully spin polarized. All Fe ions have high-spin states ($S = 5/2$). Magnetic ordering has a strong influence on the electronic structure,

while the spin-polarization splitting is almost constant. The compound is calculated to be a semiconductor with a direct energy gap of about 0.63 eV at Γ. Both the bottom of the conduction band and the top of the conduction band are mainly composed of Fe 3d states. A strong anisotropy was found from the dispersion curves, in agreement with the available data on the electrical conductivity.

Acknowledgments

Professor Dr L Feiner (UvA) and Dr H T Hintzen (TUE) are acknowledged for careful reading and useful comments on the manuscript. A part of this work belongs to the research program of the Stichting voor Fundamenteel Onderzoek der Materie (FOM), and the financial support from the Nederlandse Organisatie voor Wetenschappelijk Onderzoek (NWO) is gratefully acknowledged.

References

[1] Kojima H 1982 *Ferromagnetic Materials* vol 3, ed E P Wohlfarth (Amsterdam: North-Holland) p 305
[2] Smit J and Wijn H P J 1959 *FERRITES: Physical Properties of Ferrimagnetic Oxides in Relation to their Technical Applications* (Eindhoven: N V Philips' Gloeilampenfabrieken)
[3] Adelsköld V 1938 *Arkiv Kemi Min. Geol.* A **12** 1–9
See also Adelsköld V 1941 *Z. Kristal. Erg. Bd.* **6**
Adelsköld V 1938 *Struk. Ber.* **6** 74–5
Adelsköld V 1994 *Kirk–Othmer Encyclopedia of Chemical Technology* 4th edn, vol 10 (New York: Wiley) p 392
[4] Liu X S, Zhong W, Gu B X and Du Y W 2002 *J. Appl. Phys.* **92** 1028
[5] Pieper M W, Kools F and Morel A 2002 *Phys. Rev.* B **65** 184402
[6] Kools F, Morel A, Grössinger R, Le Breton J M and Tenaud P 2002 *J. Magn. Magn. Mater.* **242–245** 1270
[7] Heimke G 1976 *Keramische Magnete* (New York: Springer)
[8] Gorter E F 1957 *Proc. IEEE* **104B** 255S
[9] Bertaut E F, Deschamps A, Pauthenet R and Pickart S 1959 *J. Physique Rad.* **20** 404
[10] van Wieringen J S 1967 *Philips Tech. Rev.* **28** 33
[11] Lotgering F K, Locher P R and van Stapele R P 1980 *J. Phys. Chem. Solids* **41** 481
[12] Litsardakis G 1997 *J. Physique Coll.* IV **7** C1 341
[13] Zainullina V M, Zhukov V P and Zhukovskii V M 2001 *J. Struct. Chem.* **42** 705
[14] Ida K, Minachi Y, Masuzawa K, Nishio H and Taguchi H 1999 *J. Magn. Soc. Japan* **23** 1093
[15] Obradors X, Solans X, Collomb A, Samaras D, Rodriguez J, Pernet M and Font-Altaba M 1988 *J. Solid State Chem.* **72** 218
[16] Kimura K, Ohgaki M, Tanaka K, Morikawa H and Marumo F 1990 *J. Solid State Chem.* **87** 186
[17] Borown I D and Altermatt D 1985 *Acta Crystallogr.* B **41** 244
[18] Brese N E and O'Keeffe M 1991 *Acta Crystallogr.* B **47** 192
[19] van Leuken H, Lodder A, Czyzyk M T, Springelkamp F and de Groot R A 1990 *Phys. Rev.* B **41** 5613
[20] Hedin L and Lundqvist B I 1971 *J. Phys. C: Solid State Phys.* **4** 2064
[21] Andersen O K and Jepsen O 1984 *Phys. Rev. Lett.* **53** 2571
[22] Andersen O K 1975 *Phys. Rev.* B **8** 3060
[23] Shannon R D 1976 *Acta Crystallogr.* A **32** 751
[24] Bertaut E F, Deschamps A, Pauthenet R and Pickart S 1959 *J. Physique Rad.* **20** 404
[25] Zaveta K 1963 *Phys. Status Solidi* **3** 2111
[26] Wijn H P J 1970 *Numerical data and Technology* (*Landolt–Börnstein New Series* Group III vol 4b) ed K-H Hellwege (Berlin: Springer) p 552
[27] Baszynski J 1973 *Acta Phys. Pol.* A **43** 499
[28] Neumann H and Wijn H P J 1968 *J. Am. Ceram. Soc.* **51** 536
[29] Fontijn W F J, van der Zaag P J, Feiner L F, Metselaar R and Devillers M A C 1999 *J. Appl. Phys.* **85** 5100
[30] Dülken H, Haberey F and Wijn H P J 1969 *Z. Angew. Phys.* **26** 29
[31] Jones R O and Gunnarsson O 1989 *Rev. Mod. Phys.* **61** 689